«ФИЗИКА ЭЛЕМЕНТАРНЫХ ЧАСТИЦ И АТОМНОГО ЯДРА»
1992, ТОМ 23, ВЫП.4

УДК 539.172

EXPERIMENTAL NUCLEAR REACTION STUDIES AND NUCLEAR ASTROPHYSICS*

E.Somorjai

Institute of Nuclear Research of the Hungarian Academy of Sciences
Debrecen, Hungary

The main goal of the paper is to show the close relation between nuclear spectroscopy in nuclear reactions and nuclear astrophysics and to show the significance of processes being negligible among normal circumstances but astrophysical ones.

Цель работы — показать тесную связь между ядерной спектроскопией в ядерных реакциях и ядерной астрофизикой. Кроме этого, наблюдается усиление некоторых процессов в астрофизике, которые несущественны в нормальных условиях.

1. INTRODUCTION

Nuclear astrophysics is a very prosperous and fast developing field. It is a combination of astrophysics and nuclear physics. It would extend hours to mention only the most important parts of it. Therefore, in the brief time allotted here the subject should be strongly reduced. Namely, the low-energy charged-particle-induced nuclear reactions will be only discussed here. However, it turns out that from astrophysical point of view reactions of this kind (thermonuclear) are the most important ones. In stars they play leading role as sources of energy and of element synthesis.

The main goal of my talk is — without entering into details of nuclear astrophysics — to show, on the one hand, the close relation between nuclear spectroscopy in nuclear reactions and nuclear astrophysics, on the other hand, the significance of processes being negligible among normal circumstances but astrophysical ones. That aim will be fulfilled by three examples. Two of them are experimental works (with my participation during a one year study in Münster, Germany) and the additional one (taken from

*Talk given at the session «Trends in Physics» at the Hungarian Academy of Sciences (7 May, 1991)

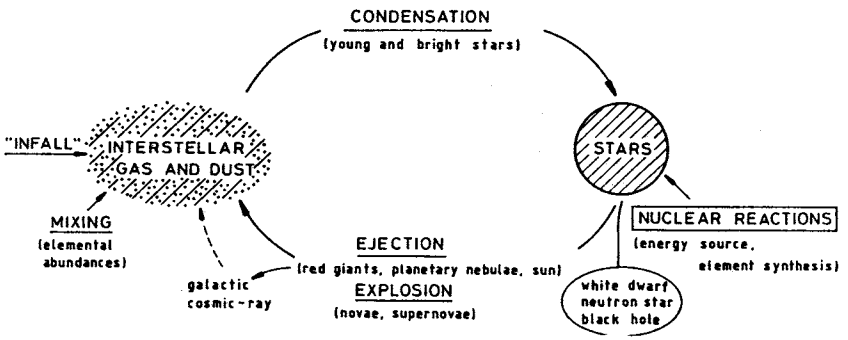

Fig.1. Schematic picture of the material circulation in a galaxy [1]

ref. [1]) is a complex, expressive consequence of selection rules in nuclear physics. Before the examples, a very short introduction-like description of the synthesis of elements and the star evolution is given together with a few basic relations in nuclear astrophysics.

The elemental abundances are the result of mixing in the course of a cyclic evolution shown in Fig.1 [2]. Some material can escape from the cycle as stellar residues (white dwarfs, etc.) or galactic cosmic-ray nuclei and, on the other hand, some material (possibly of Big Bang composition) may infall. In the cycling process the stars are the very sites for different nuclear reactions providing energy for stabilizing themselves against gravitational contraction during the different burning stages (Fig.2) of their life. A burning stage is also responsible for changes in elemental composition, while the intercurrent episodes of gravitational contraction (downward arrows on Fig.2) generate temperature increases. The general evolution of a massive ($M = 25M_{\odot}$) star is shown schematically in Fig.2 taken from ref. [3]. The figure illustrates the central temperatures, densities as well as the duration of different burning stages with the most abundant nuclei left after a given burning mode. The figure also shows that a burning phase after its completion is drawn out from the central region into a thin peripheral shell, so the deep stellar regions are similar to an onion with dufferent skins of different composition. The fate of a star is very complex (depending mostly on its mass) and a detailed treatment of that question is far beyond the scope of this talk.

All of the critical stellar features (energy production, nucleosynthesis of elements, etc.) depend directly on the magnitude of the reaction rate per particle pair, $<\sigma v>$ [2]:

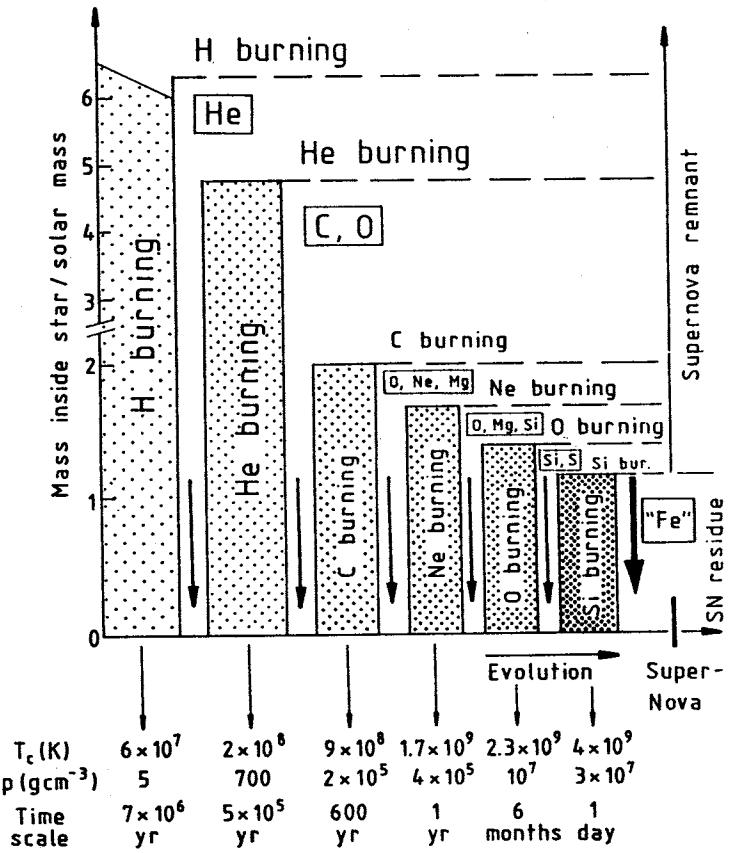

Fig.2. General evolution (schematic) of a $M = 25M_{\odot}$ star [3]

$$<\sigma v> = \left(\frac{8}{\pi M_{12}}\right)^{1/2} \frac{1}{(kT)^{3/2}} \int_0^{\infty} \sigma(E) \exp\left(-\frac{E}{kT}\right) E\, dE, \qquad (1)$$

where $<\sigma v>$ means a value averaged over the velocity distribution which is a Maxwell — Boltzman one in the case of normal stellar gas (thermodynamic equilibrium). Here T refers to the temperature of the gas, M_{12} is the reduced mass of the interacting nuclei, $E = \frac{1}{2} M_{12} v^2$ is the center-of-mass energy and $\sigma(E)$ is the reaction cross section. For nonresonant charged-particle-induced reactions the cross section can be expressed as:

$$\sigma(E) = S(E)\frac{1}{E}\exp(-2\pi\eta), \tag{2}$$

(for details see, e.g., ref. [2]), where the function $S(E)$ defined here is referred to as the nuclear or astrophysical S-factor containing all the strictly nuclear effects. The quantity η is called the Sommerfeld parameter and $2\pi\eta$ is the Gamow factor expressing approximately the tunneling probability for particles with charges Z_1 and Z_2:

$$2\pi\eta = 2\pi Z_1 Z_2 e^2/\hbar v. \tag{3}$$

Combining equations (1), (2) and (3), the reaction rate per particle pair is:

$$\langle\sigma v\rangle = \left(\frac{8}{\pi M_{12}}\right)^{1/2}\frac{1}{(kT)^{3/2}}\int_0^\infty S(E)\exp(-E/kT)\exp(-2\pi\eta)\,dE, \tag{4}$$

which is grafically shown in Fig.3 [2]. The product of the two exponential terms (hatched area) leads to a relatively narrow energy window around the effective burning energy of E_0 ($E_0 > kT$), where the nuclear reactions take place. In general, for stellar temperatures this window is far below the Coulomb barrier (e.g., $E_0 = 14.8$ keV for $^7\mathrm{Li} + p$ at $T = 15\times10^6$ K and $E_{\mathrm{Coul}} \cong 1.7$ MeV), consequently the experimental reaction cross sections are needed at very low (essentially at zero) energies. (For resonance reactions eq. (4) contains the sum of resonance strengths instead of the $S(E)$-factor [2]). The cross section $\sigma(E)$ of a charged-particle-induced reaction drops sharply with decreasing energy E for beam energies below the Coulomb barrier E_C, which means a practical lower limit E_L for cross section measurements, thus the only way is the extrapolation. Since the S-factor is a smoothly varying function of energy the advantage of using that instead of $\sigma(E)$ (eq. (2)) is obvious as it is clearly demonstrated on Fig.4 [2]. Note the logarithmic and linear scales on the upper and lower parts of Fig.4, respectively.

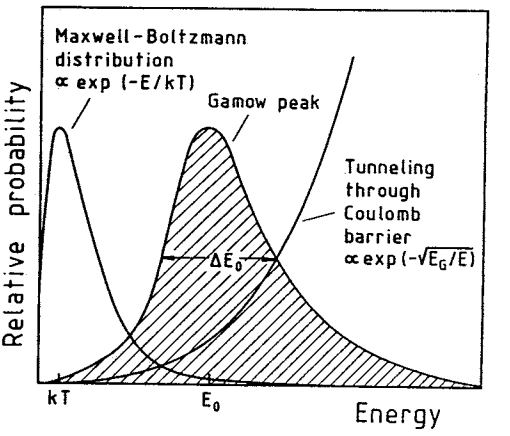

Fig.3. Schematic diagram of the effective stellar energy region for nuclear reactions between charged particles [2]

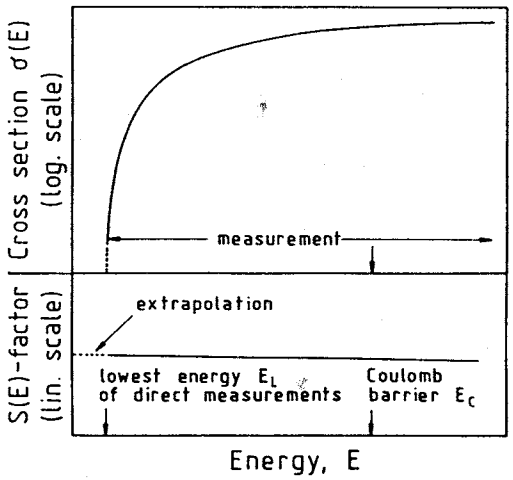

Fig.4. The energy dependence of the cross section $\sigma(E)$ and the $S(E)$-factor for a charged-particle-induced nuclear reaction [2]

Fig.5. The possible components of the $S(E)$-factor in charged-particle-induced reactions [2]

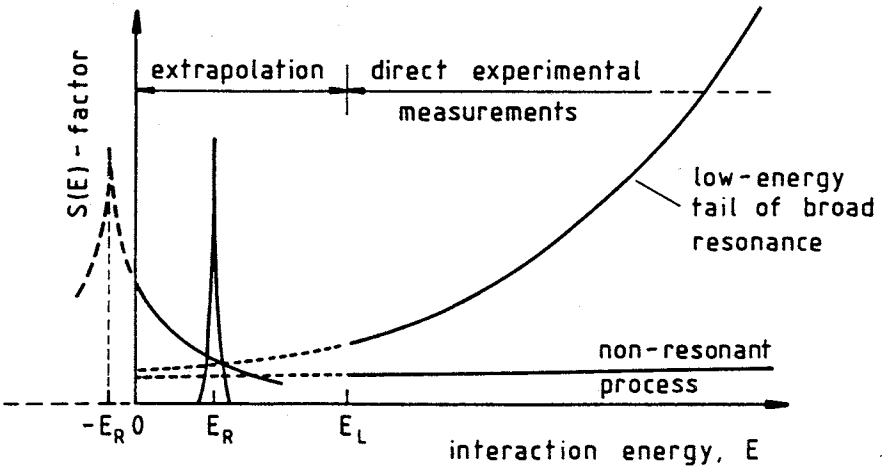

On the basis of the very short review above, one can come to the conclusion that merely the reaction cross sections are needed for the astrophysics. It is true, however, for getting reliable cross section data the full arsenal of nuclear spectroscopy has to be used. The above sketched features of nuclear astrophysics are very simplified ones, the general case is shown on Fig.5 [2]. Besides the non-resonant case, there are other processes contributing to the S-factor (or cross section), namely, resonances at higher energies (broad ones) or at lower energies (sometimes in the extrapolation region) and even below the reaction threshold. In addition interferences can frequently occur between resonant and non-resonant processes. To take all of

these phenomena into account the exact knowledge of reaction mechanism and resonances together with their parameters (J^{π}, strength, width, etc.) is necessary. For that, sometimes additional reaction(s) is to be studied too (for resonances in the extrapolation and subthreshold region).

Before turning to the examples mentioned above it should be emphasized that besides charged-particle-induced reactions, being discussed here, other reactions, like neutron capture, photodisintegration and to some extent fusion of light heavy ions, are also very important in astrophysics. However they are out of the scope of this talk.

2. ELECTRON SCREENING IN THE REACTION OF ^{6,7}Li (p, α) ^{3,4}He

As it was pointed out in the previous part, for getting the $S(E)$ value at the effective stellar energy ($\cong 0$) the experimental values should be extrapolated. To improve the extrapolated value experimentalists make every effort for performing measurements at lower and lower enegies. However, according to a prediction [4] for the cross section of reactions between light nuclei and projectiles (mostly protons) at low energies, a simple process negligible at higher energies, the electron screening becomes significant. The basic idea of that screening is the following.

In nuclear physical treatments (e.g., eqs. (2) and (3)) it is assumed that the Coulomb potential of the target nucleus as seen by the projectile is that resulting from a bare nucleus and it thus would extend to infinity. However, for nuclear reactions studied in the laboratory the target nuclei are usually in the form of atoms or molecules. The atomic (or molecular) electron cloud surrounding the target nucleus acts as a screening potential: an incoming projectile sees no repulsive Coulomb force until it penetrates beyond the atomic radius R_a, thus it effectively sees a reduced Coulomb barrier. At low projectile energies, when the classical turning point R_c of an incoming particle for the bare nucleus is near or outside the atomic radius, the magnitude of the shielding effect becomes significant: the condition $R_c \geq R_a$ leads to energies $E \leq U_e = Z_1 Z_2 e^2 / R_a$. Setting R_a equal to the radius of the innermost electrons of the target (or projectile) atoms, the resulting energies U_e are quite low (e.g., $U_e = 0.24$ keV for ^{7}Li (p, α) ^{4}He) and thus the shielding effects might really appear to be effectively unimportant. However, the penetration through a shielded Coulomb barrier at energy E is equivalent to that of bare

nuclei at energy $E_{\text{eff}} = E + U_e$. Thus the shielding effect increases the cross section with an enhancement factor f given by [4]:

$$f = \frac{\sigma(E_{\text{eff}})}{\sigma(E)} \approx \frac{E}{E_{\text{eff}}} \frac{\exp(-2\pi\eta(E_{\text{eff}}))}{\exp(-2\pi\eta(E))} \approx \exp\left(\frac{\pi\eta(E)U_e}{E}\right) \text{ for } U_e << E, \quad (5)$$

i.e., the factor f increases exponentially with decreasing energy. For energies $E/U_e \geq 1000$ the shielding effects are negligible (e.g., $f \cong 1.003$ for ^{7}Li (p, α) ^{4}He). However, at energies $E/U_e \leq 100$ the shielding effects cannot be disregarded (e.g., $f \cong 14.0$ and 1.09 at $E/U_e = 10$ and 100, respectively, for ^{7}Li (p, α) ^{4}He) and become important for the understanding of the low-energy data.

Several reactions involving light nuclides have been carried out towards, and in some cases even below, the region $E/U_e = 100$ ([4] and references therein). However, the experimental errors for these low-energy data are too large to draw any meaningful conclusions. The first real experimental evidence of the electron screening was found in the reaction ^{3}He (d, p) ^{4}He [5] and most of the theoretical calculations [5—8] underestimate the experimental data.

Here new experimental data are presented for the reaction ^{6,7}Li (p, α) ^{3,4}He [9]. The reactions were studied at the 100 kV accelerator at the Ruhr Universität Bochum (Germany), which provided beams of H_1^+, H_2^+ and H_3^+ ions at energies $E_{\text{lab}} = 20$ to 100 keV with particle current up to 3 mA at the 350 kV accelerator at the Universität Münster, which provided $^6Li^+$ and $^7Li^+$ ions at energies $E_{\text{lab}} = 77$ to 350 keV. Solid LiF targets on Ta-backing and H_2-gas targets were used. The solid targets have been fabricated with lithium of natural abundance and with lithium enriched to 99% in ^{6}Li in the cases of ^{7}Li and ^{6}Li targets, respectively. The thickness of solid targets (300 to 1000 μg/cm^2) was large enough to totally stop the incoming protons. During the course of the experiments the stability of solid targets was checked periodically: no target deterioration was observed for bombarding times of more than a week. The proton beam passed through a Cu collimator and was focused into a profile of about 1.5 cm diameter on the target. The target was mounted at 90° with respect to the beam direction. Direct water cooling was applied to the target. A liquid-nitrogen (LN_2) cooled in-line Cu tube extended from the collimator to within 3 mm of the target. The tube near the target had appropriate holes to allow the observation of reaction products in 4 Si particle detectors (active area = 450 and 600 mm^2, thickness = 500 and 100 μm)

positioned at 130° with respect to the beam direction. A negative voltage of − 300 V was applied to the tube to suppress secondary electrons from the target. The pressure in the target chamber was better than 2×10^{-6} mbar and no carbon buildup on the target was observed.

For the reverse reaction experiment a windowless gas target system of four pumping stages was used as thin H_2 target. The beam entered the rectangular target chamber through five Ta apertures and was stopped in a 20 W beam calorimeter. The gas pressure in the chamber was measured with a Baratron capacitance manometer to an accuracy of better than ±4%. The number of projectiles was measured via the calorimeter to an accuracy of ±2.5%. Two Si detectors (active area = 500 mm^2, thickness = 2000 μm) were installed in the chamber at opposite sides of the beam axis. Both in solid target and gas target experiment Ni foils were placed in front of the Si detectors to stop elastically scattered particles. In order to suppress the contribution of cosmic-ray events in the Si detectors, coincident signals from the Si detectors and a plastic scintillator (surrounding the target chamber) were rejected. Furthermore, a 5 cm thick lead shielding was placed around the plastic scintillator. Both in the solid and in the gas target cases these arrangements led to a reduction of the cosmic and room background by about a factor of 4.

The reaction yield $Y(E)$ obtained with infinite thick targets is correlated to the cross section $\sigma(E)$ [10], and the $S(E)$ factor (eq. (2)), by the relation

$$Y(E) = \int \sigma(E)\, \varepsilon^{-1} dE = \int S(E) E^{-1} \exp(-2\pi\eta)\, \varepsilon^{-1} dE, \qquad (6)$$

where the integration is carried out from zero energy to the incident beam energy and ε is the stopping power [11]. The $S_{BN}(E)$ factor for the case of bare nuclei (BN) was obtained via a polynomial fit to the previous data at higher energies [12—16] and an extrapolation down to the relevant energies of the present measurements (Fig.6). The enhancement f is then given by the experimental yield (corrected for angular distribution and target stochiometry) divided by the theoretical yield $Y_{BN}(E)$ obtained with the derived function $S_{BN}(E)$. The ratio was normalized to one at the higher energies, where no screening effects are expected. Thus, the experimental $S(E)$ factor was determined using

$$S(E) = f S_{BN}(E) = (Y(E)/Y_{BN}(E))\, S_{BN}(E) \qquad (7)$$

and is shown in Fig.6. A fit to the data using eq.(5) leads to screening potentials of U_e = 410±40 eV and 400±40 eV in the case of ^{7}Li (p, α) ^{4}He

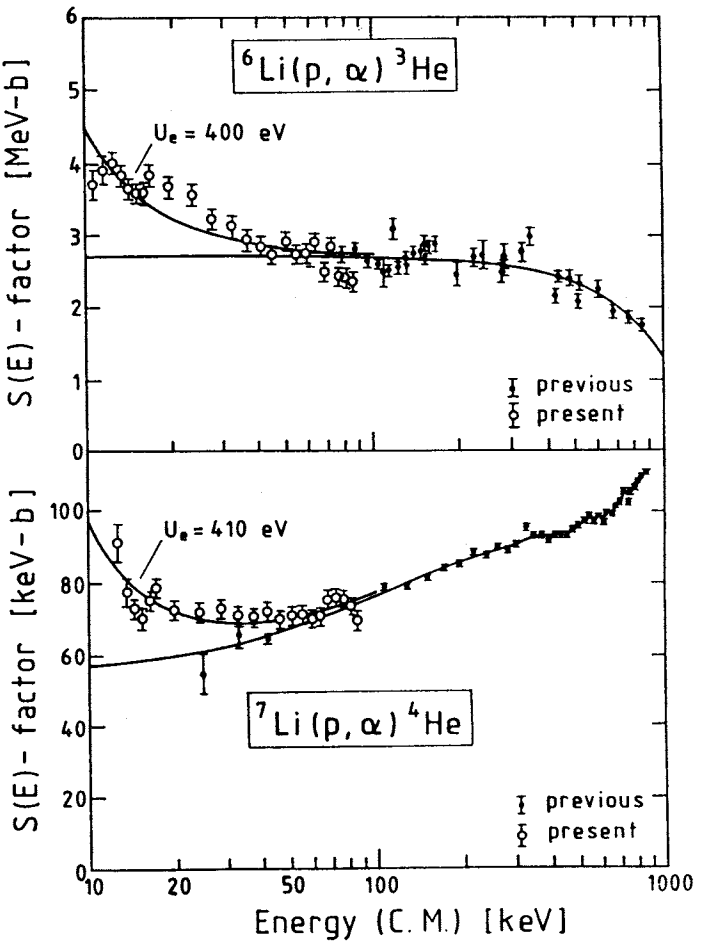

Fig.6. $S(E)$-factor data for the solid target cases. The lower curves are obtained from a fit to previous data at higher energies (see text) and are assumed to represent the case of bare nuclei. The upper curves are the calculated enhancements using eq.(5) with the fitted potentials shown on the figures

and of ^{6}Li (p, α) ^{3}He, respectively. The values are significantly higher than the expected value [4] quoted above (240 eV).

In the case of the thin H_2-gas target the corrections due to the infinitively thick targets can be avoided, otherwise the $S(E)$ values were obtained similarly to the solid target case. A fit to the data using eq.(5) leads to

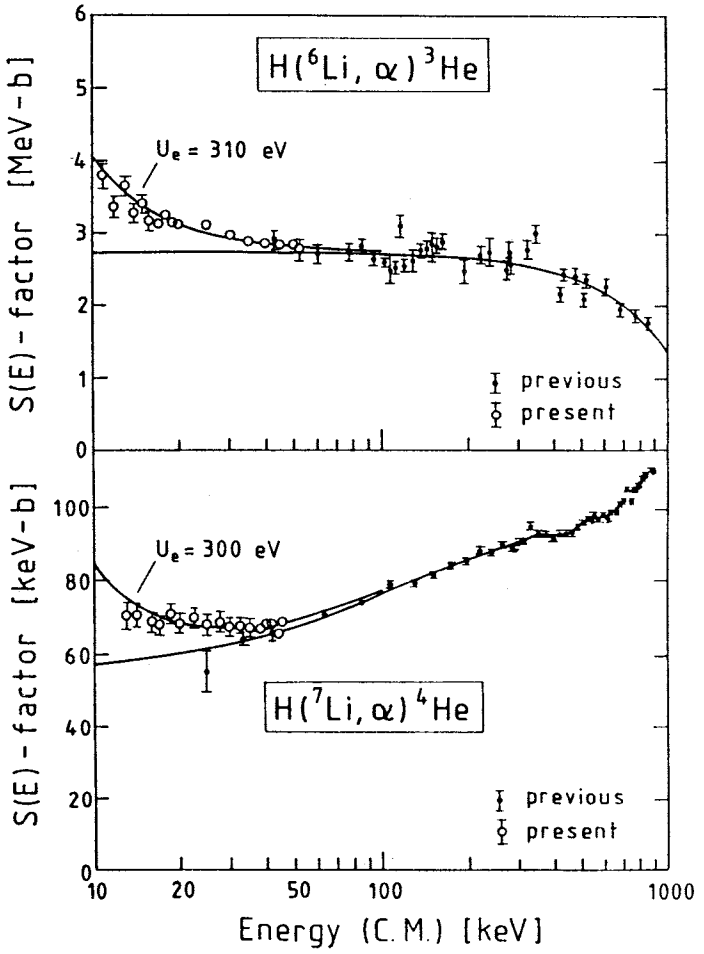

Fig.7. Same as Fig.6, for gas target

screening potentials of $U_e = 310 \pm 20$ eV for ^{7}Li (p, α) ^{4}He and $U_e =$ $= 300 \pm 20$ eV for ^{6}Li (p, α) ^{3}He (Fig.7). The values are again higher than expected.

Since the electron cloud in the H_2 molecule (gas target) is at larger distances compared to that in the H atom (projectile), the screening effect should be shifted to lower energies, i.e. U_e (H_2 + Li) < U_e (H + Li), which is qualitatively shown by our experimental values. A recent theoretical

calculation [8] strongly underestimates (U_{max} = 186 eV) the experimental values.

In summary, a good understanding of the screening effect requires additional efforts in theory as well as in experimental work, i.e., one needs improved low energy data for other fusion reactions. Such a program is in progress at the Ruhr Universität, Bochum.

3. NUCLEAR REACTION ON RADIOACTIVE TARGET: ^{22}Na (p, γ) ^{23}Mg

The main motivation of this experiment is related to the so-called «Ne — E» (E for extraordinary) problem, i.e., the discovery of neon remarkably enriched in ^{22}Ne with ^{22}Ne/^{20}Ne ≥ 0.67 (terrestrial ratio = 0.1) in the Orgueuil meteorite [18]. The results of subsequent refined measurements [19,20] and detailed nucleosynthesis calculations [21—23] have shown that the Ne — E is essentially fossil material of extinct ^{22}Na and the hot NeNa cycle (Fig.8) developing in explosive H-burning locations, and in particular in novae, could account for a sizeable ^{22}Na production. However, recent calculations [24,25] have predicted much lower ^{22}Na nova yields. This is due

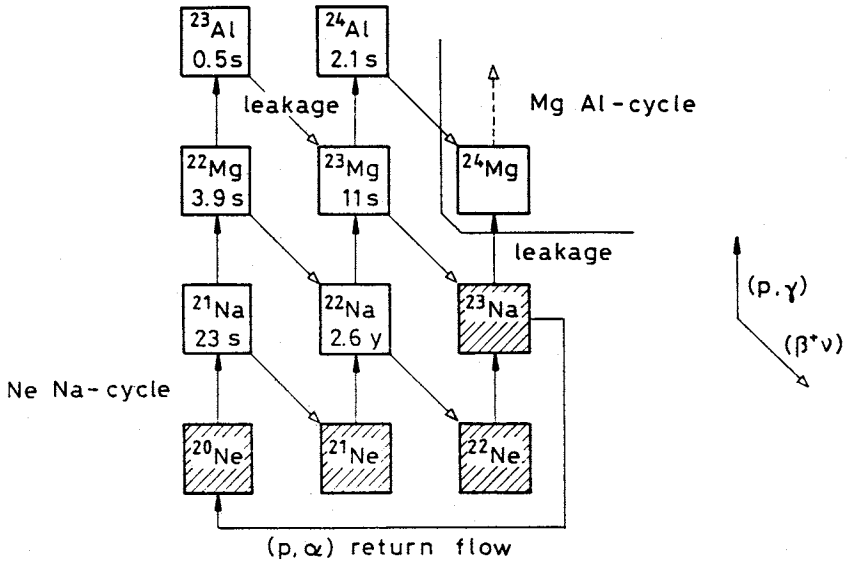

Fig.8. The sequence of nuclear reactions and β-decays in the hydrogen-burning NeNa-cycle. The half-lives of radioactive nuclides are indicated

to a large increase in the calculated reaction rates for ^{22}Na (p, γ) ^{23}Mg, which is the key reaction for ^{22}Na destruction in the hot NeNa chain [2]. The experimental work discussed below [17] gives a reevaluation of the rate of this important reaction in a range of energies (temperatures) that encompasses the most likely conditions of operation of the cold and hot NeNa chains of reactions.

The ^{22}Na (p, γ) ^{23}Mg reaction is one of examples of nuclear reactions induced on radioactive nuclei, the importance of which in the hot and explosive burning phases of stellar evolution has been addressed in recent years [26]*. It is shown on Fig.8, where the dominant stable nuclei involved in the «cold» (low-temperature) operation of the cycle are shaded. At higher temperatures, the nuclear burning times can become shorter than the half-lives; with increasing temperature the longer lived ^{22}Na nuclides (and so the ^{22}Na (p, γ) ^{23}Mg reaction) are the first to become relevant, and the cycle is said to operate in the «hot» mode. The next nucleus is the ^{21}Na, and so on.

The experimental examination of the ^{22}Na (p, γ) ^{23}Mg reaction — in addition to the already mentioned general experimental difficulties in nuclear astrophysics (low energy, small cross section) — requires a radioactive ^{22}Na target and the detection of capture gamma-rays in the presence of the «hot» target. The level diagram of the reaction is shown on Fig.9. In a previous experiment [27] only upper limits on the strengths of potential resonances were reported at $E_p^{lab} = 0.40—1.27$ MeV. Using improved experimental techniques, such as ^{22}Na mass-separator implanted targets (ISOLDE-II at CERN) and a threshold gamma-ray detector, the wide range of nuclear spectroscopy was performed for getting the necessary stellar reaction rates. For the experiment the 450 kV Sames accelerator and the 4 MV Dynamitron tandem accelerator at the Ruhr Universität Bochum provided proton beams up to 80 μA on target in the energy range $E_p = 0.17—1.29$ MeV. The beams from each accelerator were guided into the same target beam line. The beam passed through a long (1.08 m) LN_2-cooled Cu shroud with a collimator at the end of it, an electrically insulated Cu disk (with a central hole), and was finally stopped at the target. A voltage of −300 V applied to the disc was sufficient for secondary-electron suppression from both the shroud and the target. Thus, the end of the beam pipe (electrically insulated, 70 cm long)

*It should be noted that radioactive beams have the same importance with only a practical difference, i.e., for nuclei with half-life $T_{1/2} < 1h$ radioactive beam experiments, while for $T_{1/2} > 1h$ radioactive target experiments, are more advantageous [2].

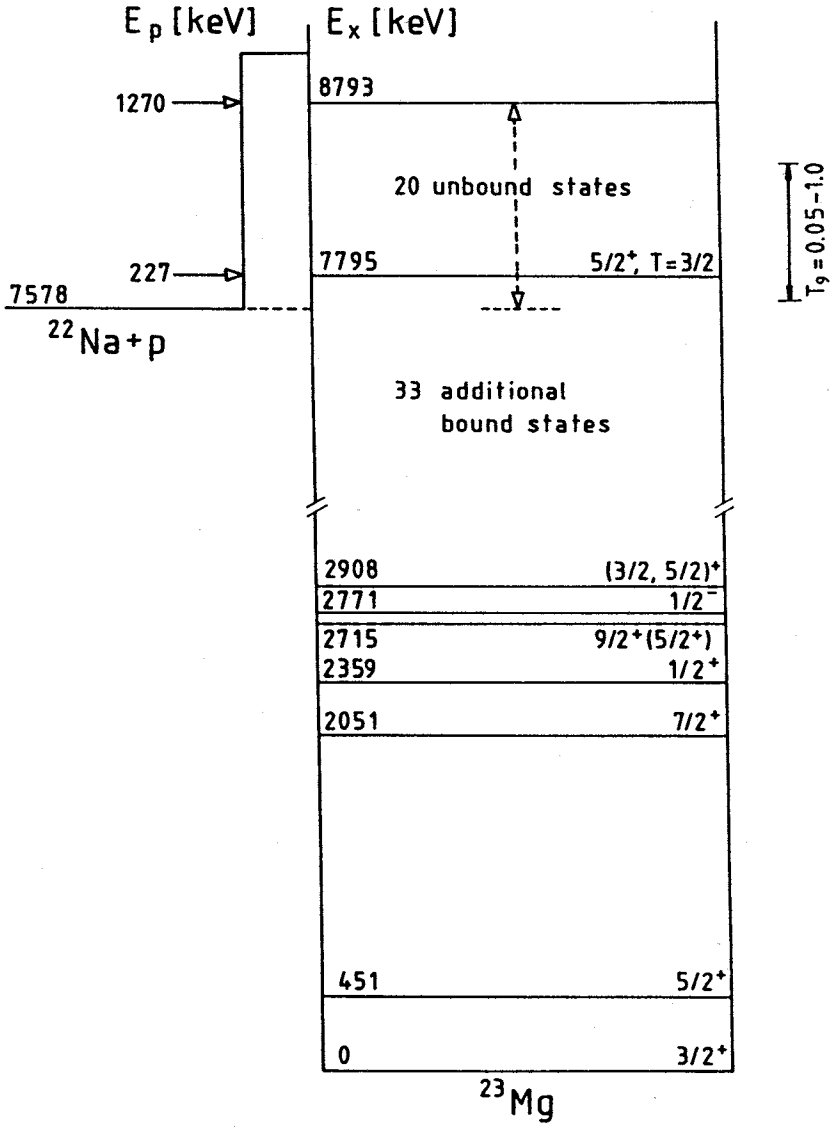

Fig.9. Level scheme of the reaction $^{22}Na(p,\gamma)^{23}Mg$. The region of astrophysical interest is indicated ($T_9 = T/10^9$ K)

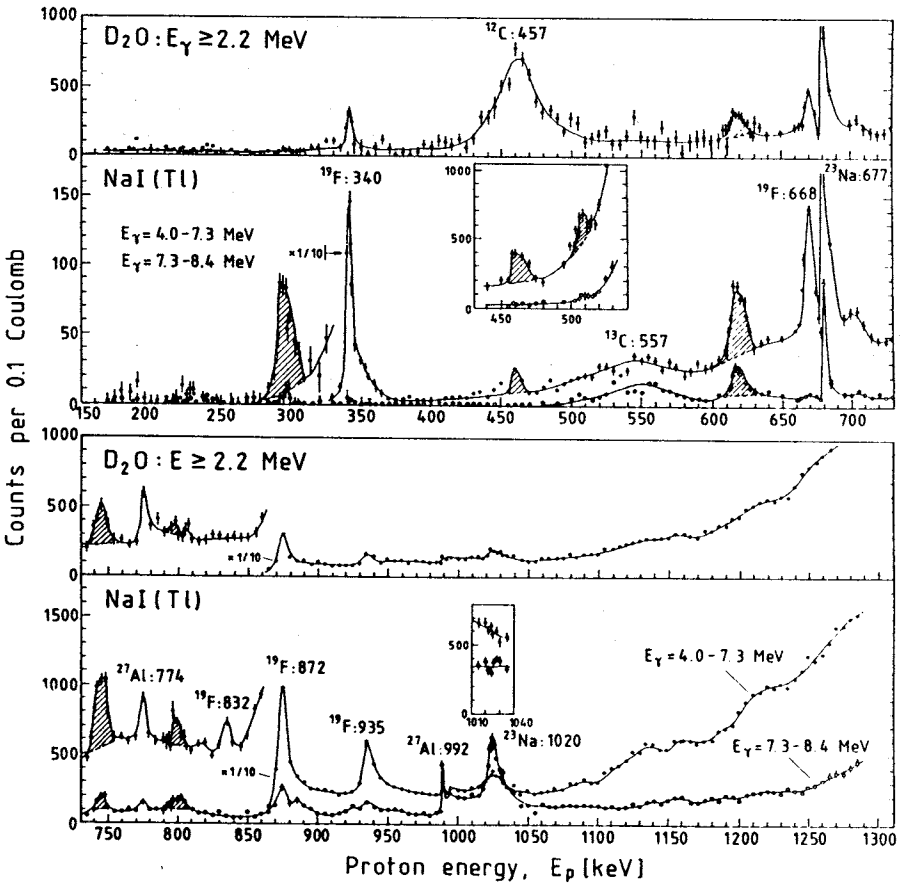

Fig.10. Excitation functions of the reaction $^{22}Na(p,\gamma)^{23}Mg$. The energy windows and detectors are indicated. The inserts show the functions taken after the bombardment with charge of 100 °C. The newly found resonances are shown by shaded structures. The curves through the data points are to guide the eyes only

together with the target formed a Faraday cup for beam integration. The targets were oriented perpendicular to the beam direction. The effective mean diameter of the beam spot was about 5 mm. In order to minimize beam-induced gamma-ray background from the shroud collimator, its beam-facing side was coated with Ni layer. The target substrates were directly watercooled. With the LN_2-cooled Cu-shroud (pressure near the target $\cong 2\times10^{-7}$ Torr) carbon deposition on the targets was strongly reduced. The implanted target

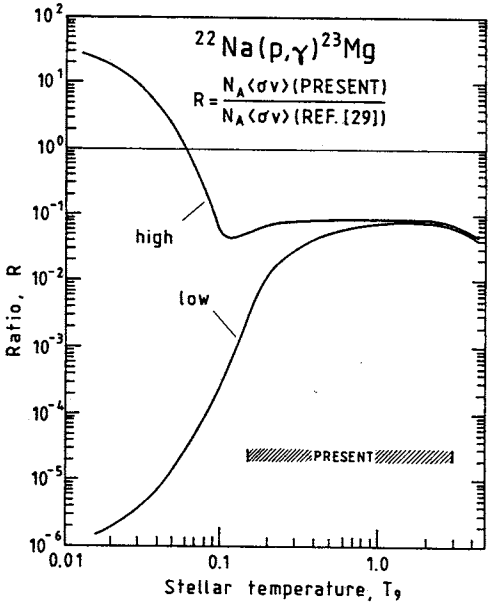

Fig.11. Ratio of the present and a previous [29] stellar reaction rates as a function of temperature. The curves labelled LOW and HIGH represent the values taken from the known resonance strengths only and from all potentially possible contributions, respectively

of 0.7m Ci ^{22}Na activity was in the form of Ni — Ta sandwich. The effective target thickness was 9 ± 1 keV at $E_p = 613$ keV.

Three different gamma-ray detectors have been used: a 7.6 cm ∅ ×7.6 cm NaI(Tl) crystal, a 145 cm^3 intrinsic Ge detector and a threshold detector of 242 l D_2O [28]. The target and the NaI crystal were installed inside a cylindrical pipe in the center of the D_2O detector. A 4.6 cm thick lead absorber between the target and the crystal gave the limit of tolerable dead-time effects (counting rate = 50 kHz). The Ge detector was placed at 0° with respect to the beam direction at a distance (and lead shield) of 6.3 cm from the target (without D_2O detector around it).

The excitation functions (Fig.10), resonance energies, resonance branching ratios, resonance strengths as well as limits of J^π assignments have been determined. From these data stellar reaction rates have been calculated. The results in comparison with an earlier estimation [29] are shown on Fig.11. The earlier overestimated values are clearly demonstrated.

Other details of our study as well as some astrophysical considerations can be found in ref. [17].

4. AN INTERESTING CONSEQUENCE OF SOME RULES OF NUCLEAR PHYSICS

(This part has been taken from ref. [1])

On the basis of many experimental studies, Fig.12 summarizes and puts in perspective the main nuclear reactions involved in quiescent He-burning in the cores of red giant stars. The ^{12}C nuclei are built with sufficient abundance

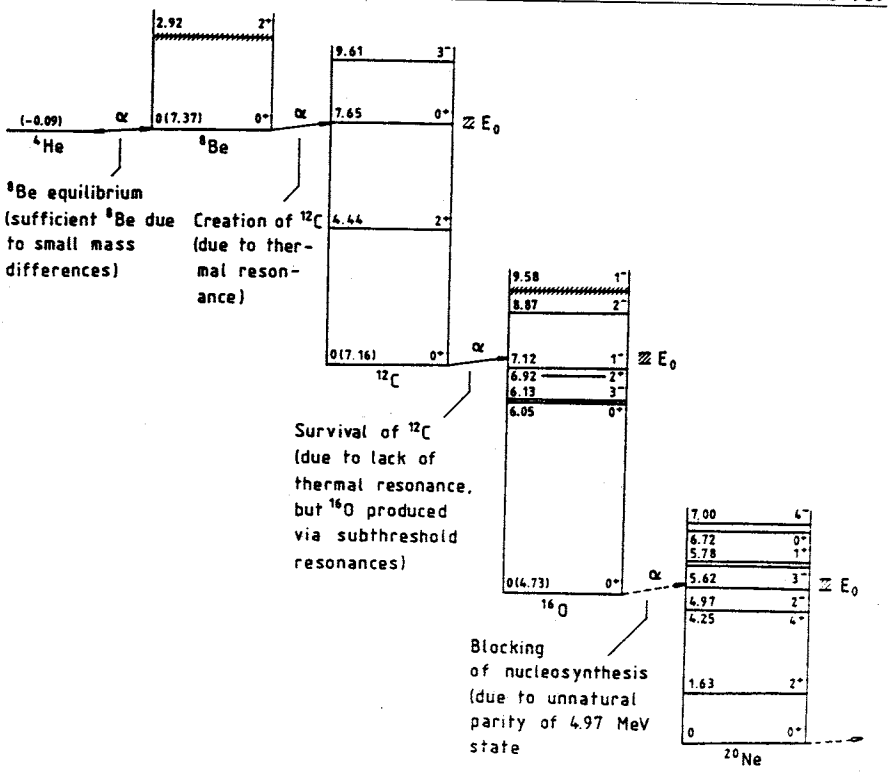

Fig.12. Level schemes of nuclei involved in the He-burning reactions in red giants [1]. The effective stellar energies (E_0) are indicated

due to small difference between the masses of a ^{8}Be nucleus and two alpha particles and a fortuitously located state in ^{12}C that provides a thermal resonance to enhance greatly the $^8\mathrm{Be}(\alpha,\gamma)\ ^{12}\mathrm{C}$ process. The resulting ^{12}C nuclei survive further bombardment with particles from the α bath due to the lack of a resonant state in ^{16}O near the most effective energy window E_0. However, the 7.12 and 6.92 MeV states provide through subthreshold resonance reactions enough yield at E_0 to let the $^{12}\mathrm{C}\ (\alpha,\gamma)\ ^{16}\mathrm{O}$ reaction proceed at a rate such that ^{12}C and ^{16}O are produced roughly in amount such that $\mathrm{C/O} \cong 0.1$. If the $E1$ gamma-decay of the 7.12 MeV state was not inhibited by isospin selection rules, ^{12}C would not have survived He-burning. The ^{16}O nuclei are not subsequently consumed because the 4.97 MeV state in

^{20}Ne, although located exactly in the most effective burning region E_0, cannot be formed via ^{16}O (α, γ) ^{20}Ne due to parity conservation. Since the nuclear properties of the 4.25 MeV state ($J^{\pi} = 4^{+}$) prevent it from acting as a subthreshold resonance, the ^{16}O (α, γ) ^{20}Ne reaction proceeds at an extremely low rate, essentially blocking nucleosynthesis via He-burning beyond ^{16}O.

As a consequence, the major ashes of He-burning in red giants are carbon and oxygen and it is generally believed that the ^{12}C and ^{16}O in galactic matter had their origin in these red giants. Both elements are also essential for the evolution of life; and it is only through some fortuitous nuclear properties and selection rules that both elements were produced so plentifully and survived the red giant phase of stellar evolution. It is perhaps instructive to speculate on how our life and the universe as a whole might have looked if the mass of ^{8}Be had not been close to the mass of two alpha particles, if there was no enhancing resonant state in ^{12}C, or if there were no parity and isospin conservation laws. Einstein is quoted as saying, «God does not throw dice». This has not been verified one way or the other; but if He (or «She») does, She (or He) is incredibly lucky.

5. SUMMARY

Here an attempt has been made to show one of the main requirements of the nuclear astrophysics, viz. many-sided knowledge of large variety of nuclear reactions. For astrophysics many nuclear reactions or processes are important in the energy range from a few keV (thermonuclear reactions) up to about 100 MeV (spallation reactions), however the low energy charged-particle-induced reactions — the subject of this review — are playing key role in the evolution of stars producing energy and being mostly responsible for elemental nucleosynthesis.

The given examples (Parts 2, 3, and 4) hopefully have proved the importance of the precise knowledge of nuclear levels (bound or resonance ones), their parameters (J^{π}, T, Γ, $\omega\gamma$, etc.) as well as the reaction mechanism. It was perhaps interesting to show how the evolution of life is determined by conservation laws of nuclear physics.

One should never forget that, because of the nature of the astrophysical problems, there are many special requirements (e.g., experiments at very low energies) and processes (e.g., electron screening) which are not encountered in ordinary nuclear physics. So, nuclear astrophysics is a great challenge for experimentalists: somehow the extreme circumstances (temperature,

density, etc.) of astrophysical sites have to be transported to the laboratory or at least be simulated. Therefore it is often a frustrating science. The desired cross sections are among the smallest ones measured in the nuclear laboratory, requiring long measuring times with scrupulously taking care of background.

At last but not least I would like to emphasize that nuclear astrophysics, in addition to the fact that it is a fast developing discipline, has also originated extremely active new fields, like experiments on «hot» targets or by «hot» beams (see e.g., [2] and references therein).

ACKNOWLEDGEMENT

Thanks are due to C.Rolfs (Bochum) for his invitation to take part in the astrophysical experiments reported here and for the excellent hospitality during that period.

REFERENCES

1. Rolfs C., Trautvetter H.P., Rodney W.S. — Rep. Prog. Phys., 1987, 50, p.233.
2. Rolfs C., Rodney W.S. — Cauldrons in the Cosmos, The University of Chicago Press, Chicago and London, 1988.
3. Arnould M., Rayet M. — Ann. Phys. Fr., 1990, 15, p.183.
4. Assenbaum H.J., Langanke K., Rolfs C. — Z. Phys., 1987, A327, p.461.
5. Engstler S., Krauss A., Neldner K., Rolfs C., Schroder U., Langanke K. — Phys. Lett., 1988, B202, p. 179.
6. Bencze Gy. — Nucl. Phys., 1989, A492, p.459.
7. Bluge G., Langanke K., Reusch H.G., Rolfs C. — Z. Phys., 1989, A333, p.219.
8. Bracci L., Fiorentini G., Melezhik V.S., Mezzorani G., Quarati P. — Nucl. Phys., 1990, A513, p.316.
9. Schroder U., Engstler S., Krauss A., Neldner K., Rolfs C., Somorjai E. — Nucl. Instr. and Meth., 1989, B40/41, p.466.
10. Gove H.E. — Nuclear Reactions, eds. P.M.Endt and P.B.Smith, North-Holland, Amsterdam, 1959, vol.1, p.259.
11. Andersen H.H., Ziegler J.F. — Hydrogen — Stopping Powers and Ranges in all Elements, Pergamon Press, New York, 1977.
12. Rolfs C., Kavanagh R.W. — Nucl. Phys., 1986, A455, p.179.
13. Gemeinhardt W., Kamke D., Rhoneck C. — Z. Phys., 1966, 197, p.58.
14. Spinka H., Tombrello T.A., Winkler H. — Nucl. Phys., 1971, A164, p.1.
15. Elwyn A.J., Holland R.E., Davids C.N., Meyer-Schutzmeister L., Mooring F.P., Ray W. Jr. — Phys. Rev., 1979, C20, p.1984.
16. Shinozuka T., Tanaka Y., Sugiyama K. — Nucl. Phys., 1979, A326, p.47.
17. Seuthe S., Rolfs C., Schroder U., Schulte W.H., Somorjai E., Trautvetter H.P., Waanders F.B., Kavanagh R.W., Ravn H., Arnould M., Paulus G. — Nucl. Phys., 1990, A514, p.471.
18. Black D.C. — Geoch. Cosmoch. Acta, 1972, 36, p.347.
19. Jungck M.H.A., Eberhardt P. — Meteoritics, 1979, 14, p.439.
20. Eberhardt P., Jungck M.H.A., Meier I.O., Niederer F.R. — Geoch. Cosmoch. Acta, 1981, 45, p.1515.

21. **Arnould M., Beelen W.** — Astron. Astrophys., 1974, 33, p.215.
22. **Arnould M., Norgaard H.** — Astron. Astrophys., 1978, 64, p.195.
23. **Clayton D.D., Hoyle F.** — Astrophys. J., 1976, 203, p.490.
24. **Woosley S.E.** — Nucleosynthesis and Chemical Evolution, eds. B.Hauck, A.Maeder and G.Meynet, Observatoire de Geneva, 1986, p.1.
25. **Wiescher M., Görres J., Thielemann F.K., Ritter H.** — Astron. Astrophys., 1986, 160, p.56.
26. **Fowler W.A.** — Rev. Mod. Phys., 1984, 56, p.149.
27. **Wiescher M., Görres J., Kratz K.L., Leist B., Chang K.H., Filippone B.W., Mitchell L.W., Savage M.J., Vogelaar R.B.** — Nucl. Instr. Meth., 1988, A267, p.242.
28. **Seuthe S., Becker H.W., Rolfs C., Schmidt S., Trautvetter H.P., Kavanagh R.W., Waanders F.B.** — Nucl. Instr. Meth., 1988, A272, p.814.
29. **Wiescher M., Langanke K.** — Z. Phys., 1986, A325, p.309.